aerospace

MDPI

Article

Conceptual Design of a Hydrogen-Hybrid Dual-Fuel Regional Aircraft Retrofit

Ulrich Carsten Johannes Rischmüller *, Alexandros Lessis, Patrick Egerer and Mirko Hornung

Bauhaus Luftfahrt e. V., Willy-Messerschmitt-Straße 1, 82024 Taufkirchen, Germany
* Correspondence: carsten.rischmueller@bauhaus-luftfahrt.net

Abstract: A wide range of aircraft propulsion technologies is being investigated in current research to reduce the environmental impact of commercial aviation. As the implementation of purely hydrogen-powered aircraft may encounter various challenges on the airport and vehicle side, combined hydrogen and kerosene energy sources may act as an enabler for the first operations with liquid hydrogen propulsion technologies. The presented studies describe the conceptual design of such a dual-fuel regional aircraft featuring a retrofit derived from the D328eco under development by Deutsche Aircraft. By electrically assisting the sustainable aviation fuel (SAF) burning conventional turboprop engines with the power of high-temperature polymer-electrolyte fuel cells, the powertrain architecture enables a reduction of SAF consumption. All aircraft were modeled and investigated using the Bauhaus Luftfahrt Aircraft Design Environment. A description of this design platform and the incorporated methods to model the hydrogen-hybrid powertrain is given. Special emphasis was laid on the implications of the hydrogen and SAF dual-fuel system design to be able to assess the potential benefits and drawbacks of various configurations with the required level of detail. Retrofit assumptions were applied, particularly retaining the maximum takeoff mass while reducing payload to account for the propulsion system mass increase. A fuel cell power allocation of 20% led to a substantial 12.9% SAF consumption decrease. Nonetheless, this enhancement necessitated an 18.1% payload reduction, accompanied by a 34.5% increment in propulsion system mass. Various additional studies were performed to assess the influence of the power split. Under the given assumptions, the design of such a retrofit was deemed viable.

Keywords: aircraft retrofit; conceptual aircraft design; dual-fuel aircraft; high-temperature hydrogen fuel cell; liquid hydrogen; hybrid aircraft; D328eco

Citation: Rischmüller, U.C.J.; Lessis, A.; Egerer, P.; Hornung, M. Conceptual Design of a Hydrogen-Hybrid Dual-Fuel Regional Aircraft Retrofit. *Aerospace* **2024**, *11*, 123. https://doi.org/10.3390/aerospace11020123

Academic Editor: Konstantinos Kontis

Received: 15 December 2023
Revised: 27 January 2024
Accepted: 29 January 2024
Published: 31 January 2024

1. Introduction

To achieve the desired reduction in climate impact of the aviation sector, formulated by e.g., the European Commission's Strategic Research and Innovation Agenda [1], all available short and long-term options need to be taken into consideration. One of the short-to-midterm approaches could be the retrofit of existing aircraft with advanced propulsion technology to reduce the pressure of entirely new clean-sheet designs with their given financial risk.

In times of intense discussions on different propulsion system concepts for varying aircraft sizes and design ranges to reduce aviation's climate impact, aircraft manufacturers are confronted with a large spectrum of available options. Next to the technological decision to be made on the powertrain configuration, and especially the energy source used, the decision on clean-sheet design or retrofit needs to be answered. For a small company as Deutsche Aircraft GmbH (DA) with its Dornier Do 328 (D328) aircraft, the retrofit approach enables the possibility to offer customers a more sustainable variant of the original product without the requirement of costly designing and certifying an entirely new product. Obviously, a retrofit will never be an entirely optimized product, but its advantages might outweigh the drawbacks by far if the correct requirements are put into

place. This is especially valid if the service life of an aircraft can be substantially prolonged by fitting a new propulsion system.

Aircraft retrofits have been investigated for decades, as they are not only an option to broaden the spectrum of sellable products but are also a valuable possibility to generate test aircraft for system tests with existing equipment. One famous example of an early liquid hydrogen (LH_2) test in aviation propulsion is the Tupolev-155, built in the 1980s, which was a retrofitted Tupolev-154 with a cryogenic tank to burn different gases in modified engines [2]. As it still used kerosene for two of the three engines, it was an early example of a dual-fuel retrofit. More recently, Universal Hydrogen demonstrated a single-side turboprop retrofit that displayed a hydrogen fuel cell (FC) rather than a hydrogen combustion engine [3]. Nevertheless, as this aircraft features no built-in LH_2 tank but rather uses loadable containers as well as uneven propeller sizes, it is seen more as a flying system testbed. The importance of hydrogen FC-electric retrofits is underlined by companies, such as ZeroAvia [4], specializing in aircraft retrofits only.

Retrofit studies have been performed on various propulsion system designs including battery-hybrid [5,6], pure FC-electric or pure hydrogen combustion (both [7]), or conventional engine replacement [8], and have also been assessed in terms of costs [9]. Hydrogen produced from renewable energy is seen as one of the key enablers of the commercial aviation sector transition to climate neutrality, with an estimated global hydrogen aircraft market value of $23.71 billion in 2030 already and a projection to reach $144.53 billion by 2040 [10]. Even though it has a potentially lower energy density compared to kerosene, depending on storage efficiency, hydrogen enables the integration of respective FCs. Nevertheless, the storage mass needs to be carried the entire mission, making the aircraft heavier than a purely kerosene-driven aircraft. Compared to the widely investigated use of batteries with their lower gravimetric energy density, hydrogen FCs require only one redox partner to be carried and reduce the fuel—and thus the mass—carried during the flight. Thermal management challenges arising due to the comparably low efficiency need to be tackled by an aerospace-tailored design of multiple components.

The project 328H2-FC, funded by the German Federal Ministry for Economic Affairs and Climate Action under the German Aviation Research Program, aims at closing the research gap for in-flight hardware tests on a retrofitted D328 using a combination of typical turboprop engines and Megawatt-scale hydrogen FC power with identical propulsion systems on each side. Due to safety aspects, this demonstrator aircraft is fitted with an additional propeller per side to house the electric motors driven by electric power from the FCs. This enables portions of the cruise to be flown hydrogen-electric only, thereby reducing emissions in the most climate-critical altitudes.

The presented retrofit study builds upon this concept but puts it into perspective for an assumed entry into service (EIS) in the year 2035 to enable an in-depth concept evaluation for a product rather than a demonstrator. The concept is based on the newer D328eco currently under development, as it features state-of-the-art engines capable of burning 100% sustainable aviation fuel (SAF) and has a longer fuselage designed for up to 40 passengers (PAX). The aim of these studies on a high-temperature FC and turboshaft engine dual-fuel parallel-hybrid concept is to develop aircraft sensitivities based on different propulsion system configurations to be able to derive powertrain requirements for future research and development activities. The selected approach features a dual-fuel parallel-hybrid propulsion system with one propeller on each side of the aircraft and turboshaft (TS) engines operating alongside hydrogen fuel cells. Rather conservative powertrain component assumptions were used to perform a realistic design space exploration for this regional CS25 turboprop aircraft retrofit. The lower bound for hybridization and technology options is estimated by studies on a minimum viable product with requirements on minimum range and PAX number. Nevertheless, these studies do not aim for a climate assessment or statements concerning hydrogen availability at relevant airports, as this is a purely aircraft-based analysis. Yet, they are part of the overall project scope.

1.1. Retrofit Concept

The Cambridge Dictionary defines a retrofit as "an occasion when a machine is provided with a part [. . .] that the machine [. . .] did not have when it was built" [11]. Following this exact definition, the presented studies deal with the topic of conceptually equipping a D328eco regional turboprop aircraft with an alternative propulsion system without altering the structure of the baseline aircraft.

On the technical side, an aircraft retrofit comes with several challenges. As the aerodynamic surfaces (wings and empennage), as well as the fuselage's external shape, may not be altered, the maximum takeoff mass (MTOM), as well as the center of gravity (CG), must stay constant. Slight changes in the CG are acceptable if the stability and maneuverability of the aircraft can be ensured. Nevertheless, CG changes will increase the trim drag of the aircraft and should, therefore, be kept at a minimum. The MTOM must not be exceeded as the structural margin for hard landings would be infringed upon or, generally speaking, the reengineering of specific parts would be required. The nacelles and propellers are allowed to be modified as long as the maximum wing-mounted mass is not exceeded. Otherwise, wing-root reinforcements would be necessary, leading to modifications in the fundamental structure of the aircraft and straying from the retrofit strategy.

For the study at hand, the choice of a retrofit allowed for a very good comparison of the performance characteristics of the hydrogen-hybrid powertrain compared to the conventional turboprop engines, as the underlying aircraft structure remained unchanged. No propulsion technologies with high modeling uncertainties were considered, e.g., distributed propulsion with its propeller-wing interaction.

A major challenge lies in the placement of the liquid-hydrogen tank due to its large volume and mass. Clean-sheet designs often assume a placement behind the aft pressure bulkhead to use the available space in the rear of the aircraft. This is especially tempting for the D328eco, as the rear part of the fuselage only contains the cargo area. Nevertheless, for a retrofit, this directly interferes with the CG requirements, if not counterbalanced. One option would be the placement of the fuel cells in the forward part of the aircraft as a counter mass. However, this introduces long, inefficient, and heavy power transmissions to the nacelles as well as large bending stresses on the fuselage. Moreover, the incorporation of an effective thermal management system poses a significant challenge, particularly when striving to maintain structural stability by avoiding the introduction of new openings for heat exchangers in the aircraft fuselage.

The chosen solution places the hydrogen tank in the cabin space close to the CG. This facilitates the aircraft design assessment but imposes challenges on the cabin design and safety. For further details, as well as possible solutions, see Section 2.2.4. Lastly, this also implies that this retrofit concept only works with a reduction in passengers and thus payload, not only due to mass but also due to space restrictions imposed by the fixed fuselage dimensions.

1.2. Hybrid Powertrain Concept

The retrofit concept not only implies challenges and restrictions to the mass and CG location but also on the available options to integrate hydrogen fuel cells (FCs) into the powertrain of the aircraft. One of the most challenging parts of the integration of FCs into an aircraft is the thermal management system (TMS) with its heat exchangers (HEXs). The latter needs to be placed in the free stream of the ambient air, drastically reducing the available placement options of the FCs, if long coolant pipes or additional openings in the fuselage are to be disregarded. Even though an integration of the FCs inside the fuselage would be possible, the thermal effect on the structure, as well as the combined CG and drag variations, impose severe challenges on other aircraft design aspects. Especially, the LH_2 tank—possibly the largest retrofitted mass depending on other powertrain component assumptions—should be placed close to the CG, allowing no room for FCs to be positioned at the same location without obstructing the passenger cabin entirely.

Therefore, the most promising solution was deemed by placing the LH_2 tank close to the CG inside the passenger cabin and the remaining systems within the nacelles located at the same wing position as the reference aircraft D328eco. For further details on the LH_2 tank and the propulsion system setup refer to Section 2.

The chosen solution is a dual-fuel parallel-hybrid propulsion system with one propeller per aircraft side and TS engines working in parallel with hydrogen fuel cells. A schematic overview of the powertrain is depicted in Figure 1 below.

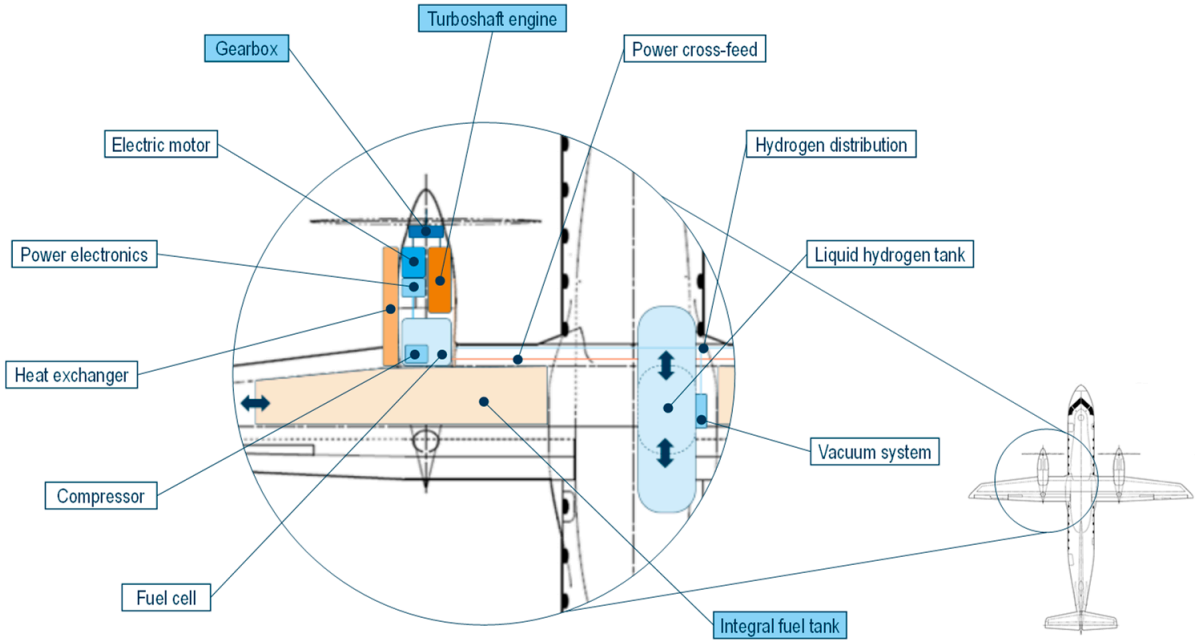

Figure 1. Schematic component overview of parallel-hybrid powertrain. Component descriptions of conventional turboprop aircraft are marked in blue.

The TS engine is located within the nacelle and is fed by fuel from the wing integral tank. Depending on the power fraction of the FC, the fuel quantity in the wing tank can easily be adjusted without modifications to the structure, as with conventional aircraft. The parallel use of the TS engine and FC allows the TS engine to be downscaled. For the study at hand, it is operated at 100% SAF.

The FC provides electrochemical power to the propeller via the power electronics (PE), the electric motor (EM), and the gearbox (GB). The latter is a two-shaft GB with entry shafts from the EM and the TS engine, combining their power to fulfill the propeller requirements. Hydrogen is fed through pipes from the LH_2 tank to the FCs via the fuselage and wing, where it is converted to electric power using air (oxygen) from an aerospace-tailored compressor. The systems within the nacelle also include the TMS with its HEX providing the required cooling capability for the EM, PEs, and FCs.

Finally, a power cross-feed provides the required redundancy to direct electric power from one nacelle to the other in case of a major malfunction.

2. Aircraft Design Methodology

As the presented work is a purely theoretical study, modeling the conceptual aircraft within the Bauhaus Luftfahrt Aircraft Design Environment (BLADE) was a fundamental component of the study-related work. A detailed explanation of the overall BLADE aircraft design methodology and subsequent aircraft derivatives can be found in [12]. BLADE primarily employs semi-empirical methods for aircraft sizing, focusing on mass estimation, aerodynamics, and overall aircraft performance [12–15], and is designed to interact with a CPACS (Common Parametric Aircraft Configuration Schema, [16]) representation of the aircraft. Nevertheless, specific areas of interest are addressed using physics-based or

analytical methods, including the assessment of the engine and fuel cell performance, as well as the hydrogen tank mass and thermodynamic calculations. All relevant assumptions and parameters need to be reflected within the model to allow the derivation of sensitivities for certain aspects of the design. This is especially relevant for the propulsion system, being therefore introduced in detail alongside its sizing logic and a general introduction to the hybridization strategies.

For the setup and calibration of the conceptual aircraft, a reference aircraft approach was used [12]. This allowed us to derive a sophisticated model of the year 2035 retrofit. Finally, the overarching BLADE setup is introduced in the last section of this chapter.

2.1. Reference Aircraft

The previously introduced D328eco functions as the reference aircraft in the subsequent studies. Currently undergoing development by DA and originating from the Dornier Do 328, it serves as the focal point for investigation. The aircraft features a 3-seat abreast configuration with the aisle splitting it into a 1-seat and 2-seat side. Several modifications are being implemented in comparison to the D328. Besides introducing modern avionics and new landing gear, new powerplants are also being installed. The aircraft will be equipped with two PW127XT-S engines designed to be fully SAF compatible (for more details on the propulsion system, refer to Section 2.2.1). Furthermore, comprehensive redesign efforts are being directed towards the fuselage and cabin. The fuselage of the D328eco represents an elongated iteration of the D328, featuring an augmented standard seating capacity accommodating up to 40 passengers. Visualizations of the D328eco can be found in Figure 2 and further key specifications of the D328eco can be found in Table 1.

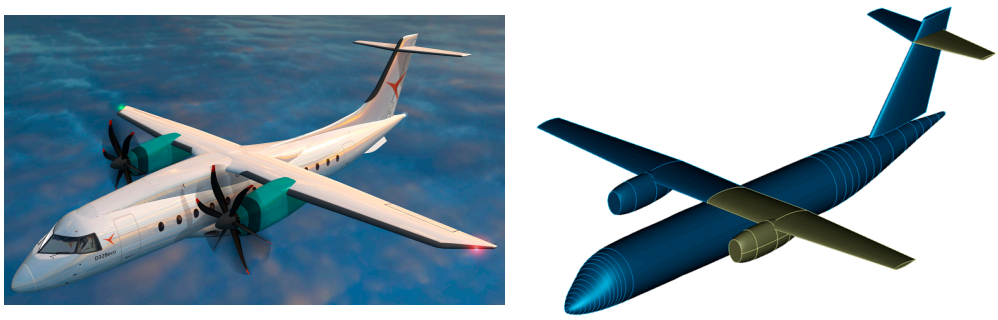

(**a**) (**b**)

Figure 2. Visualizations of (**a**) the D328eco according to DA [17] and (**b**) BLADE CPACS.

Table 1. D328eco reference aircraft specifications & top-level aircraft requirements.

D328eco Specifications	Value	Unit
Entry into service	2026	Year
Length	23.30	m
Span	20.98	m
Maximum takeoff mass	15,660	kg
Maximum takeoff power [1]	2048	kW
Propeller diameter	3.96	m
Top-level aircraft requirement		
Design range	580	NM
Design payload [2]	3880	kg
Cruise Mach number	0.49	-
Cruise altitude	27,000	ft
Takeoff field length	1234	m

[1] With PW127XT-S engines installed, per engine. [2] With 40 PAX @ 97 kg.

This table also presents the top-level requirements for the aircraft (TLARs). While configuring the design mission, the payload mass was established at the equivalent mass of 40 PAX, aligning with an assumed seat load factor of 100%. The associated design range is extrapolated from a targeted payload-range capability provided by DA. It is imperative to underscore that the design mission, along with all ensuing studies, was calculated under ISA conditions.

2.2. Models & Methods

This section describes the models and methods for the conceptual aircraft design with their coupled assumptions for the major parts of the propulsion system. The TS engine still holds the largest power fraction provided to the propellers but is now supported by hydrogen FCs. The FC operation is adjusted independently for each flight point. A TMS and an LH_2 tank are required to operate the FCs, forming the core of the dual-fuel hydrogen-hybrid powertrain concept together with the other components.

2.2.1. Turboshaft Engine, Gearbox & Propeller

For the presented studies, tabulated off-design engine-performance data for the PW127XT-S turboprop engine was derived from a generic turboshaft engine deck. It was split into a turboshaft deck and a propeller deck. Both decks were discretized based on rating, altitude, Mach number, and shaft power. The propeller deck incorporated thrust as an additional dimension, while the turboshaft deck included values for both fuel flow and exhaust thrust. Each deck contained more information, but only the aforementioned fields were extracted and utilized. This tabulated data was then interpolated for each flight point and the engine performance characteristics were determined and used in the mission calculation. To model the engine characteristics for different design points, the decks were scaled accordingly, based on a reference design point. The split into two decks also allowed for independent scaling between the propeller and turboshaft and thus enabled their use in a hybrid powertrain model, where the propeller might be powered by two or more independent power-delivery systems.

To define the powertrain design point, a total aircraft thrust was specified, and the propeller thrust, shaft power, and exhaust thrust were iterated to ensure that the combined propeller and exhaust thrust met the specified aircraft thrust requirement. The powertrain design point for the reference aircraft was chosen in a way that the originally provided data was preserved without any modifications, thereby ensuring the utilization of the reference engine's performance characteristics.

Regarding mass calculations, the powertrain of the reference aircraft included a turboshaft, gearbox, subsystems, a nacelle structure, and a propeller. The mass of the turboshaft was computed following the methodology outlined in [18], while the gearbox mass was determined using the approach detailed in [19]. Both of these methods depended on the sea-level maximum shaft power that the turboshaft could provide. The gearbox mass also depended on the turboshaft and propeller shaft rotational speeds, which were derived based on [20]. The nacelle structure and propeller masses, as well as the nacelle size, were modeled to vary with the powertrain design thrust and power. These regressions were calibrated to match the reference aircraft component masses and dimensions.

The subsystems are regarded to be powered by the turboshaft engine via an accessory gearbox. No power-offtake calculations were performed, as the additional fuel consumption and power increments related to the subsystems were accounted for in the turboshaft deck. The mass of these subsystems was assumed to be independent of the powertrain design point and therefore the reference aircraft subsystems mass was used for all aircraft variations. As this paper specifically focuses on a retrofit variant, examining the interdependency between powertrain size and subsystems falls outside the scope of the presented studies.

2.2.2. High-Temperature Polymer-Electrolyte Fuel Cell

For the presented study, the type of fuel cells was chosen according to a multitude of criteria derived from the aircraft's operational requirements. The operational temperature, the power density, specific power, system efficiency, and response time during load changes were all taken into consideration, only to name a few. Based on these requirements, solid-oxide fuel cells (SOFCs) were disregarded, mainly due to their slow response time and delicate operational behavior as well as their air inlet requirements. Conventional polymer-electrolyte membrane fuel cells (PEFCs) have a good response time and show a good performance for the expected load cycle, but come with the drawback of a low temperature difference between its operating temperature, of around 80 °C, and the ambient air [21–23]. As the aircraft design was only performed using ambient air to cool the systems, the use of high-temperature polymer-electrolyte fuel cells (HT-PEFCs) with an operating temperature of up to 220 °C was chosen. The higher temperature largely increased the temperature spread and, thus, alleviated the performance requirements of the thermal management system (TMS) due to increased thermal efficiency. Details of the TMS design can be found in Section 2.2.3. The FC degradation effects were not considered [24].

The FC model is based on the performance and hydrogen flow characteristics of the low-temperature 2017 Toyota Mirai FC [25], adjusted towards the performance characteristics of an HT-PEFC operating at 220 °C. The FC system performance characteristics include all the balance of plant (BoP) system offtakes, apart from the compressor. Even though a lower BoP power consumption may be expected due to the water management being superfluous for an HT-PEFC, it remained unchanged.

To properly mimic the behavior of the reference FC characteristics, so-called virtual stacks were introduced. The virtual stack number was obtained by dividing the maximum power requirement of the FC system by the maximum power output of the reference FC stack. The virtual number of stacks could be a decimal number and was therefore amended by the term virtual, as it was purely a number used for correct system sizing and behavior representation. By following this approach, the correct scaling of non-linear stack parameters as the hydrogen flow or the system efficiency over power was ensured irrespective of the actual FC system power demand. These stack-dependent characteristics were derived from [25], and amended by a specific FC idle rating to ensure a proper idle state for flight phases with low power requirements on the FC.

To account for the increasing compressor power consumption for higher altitudes, the maximum internal FC power was kept constant, but its power output to the propulsion system was reduced by the respective amount required by the compressor. This also ensured the correct FC hydrogen flow with respect to altitude and propeller power demand. The mass of the aerospace-tailored compressor, with respect to its maximum power consumption, was calculated according to a heuristic from [26,27], and its power consumption was assumed to be an increasing quadratic variation with altitude up to FL270 as shown in Equation (1)

$$P_{Compressor}\,[kW] = P_{FC}\,[kW] * (7 \times 10^{-9} * \text{Altitude}\,[ft]^2 + 8 \times 10^{-5} * \text{Altitude}\,[ft])/100 \quad (1)$$

according to a BHL-internal assessment.

It was refrained from using a buffer battery due to a multitude of reasons. Omitting a battery reduced the mass and system complexity, facilitated system behavior modeling, disabled quick turnarounds due to expectable charging times, and sharpened the focus of the studies on the TS-FC interaction. Certainly, it decreased the hybridization strategy options but therefore enabled us to draw a clearer picture of the expected drawbacks and benefits of this type of retrofit. Additionally, there was no mass reduction potential for batteries during cruise, which comes into play for longer missions. In particular, however, the dynamic behavior of FCs in the year 2035 was deemed sufficient to form a solid response time during power changes in conjunction with the TS engine, especially as the latter holds the larger power share and has its certified dynamic properties.

For this retrofit concept, the waste products of the FC system were not further utilized. The oxygen-depleted air, as well as the water vapor, are simply discharged via exhaust pipes into the ambient air, creating no additional thrust or drag. The vapor enhances contrail formation depending on the atmospheric conditions [28], but as climate assessments were not part of these studies, no further insights were generated. Additionally, condensing liquid water out of the exhaust vapor was disregarded as this is a retrofit study, and it refrained from altering the structure and systems of the aircraft to accommodate this. The waste heat of the FC stacks was purely directed to the heat exchangers (HEXs), where it was discharged to the ambient air. Numerous utilization possibilities could be considered but were not the focus of these studies and were therefore neglected. Examples include nacelle and wing leading-edge anti-ice systems, environmental control system (ECS) heating, or hydrogen system component heating.

2.2.3. Thermal Management System

Given its substantial impact on the overall performance of the hybrid-electric powertrain, considerable attention was dedicated to the examination of the thermal management system in this study. At BHL, the in-house developed, python-based fluid simulation environment ICCE (Innovative Cooling Concept Environment, [29]) is being used to perform all relevant TMS calculations. It incorporates fluid and fin databases, and a core library defines the microscopic geometry of the heat exchanger surface on the hot and cold sides. As a modular thermodynamic cycle program, it provides the ability to combine various TMS-specific components into the desired cooling system setup, making it adjustable to numerous aircraft-specific cooling problems. The components include, but are not limited to, pumps, pipes, nozzles, diffusers, fans, cooling liquids, and heat exchangers (HEXs). They are sized using a multipoint design strategy for hot-and-high takeoff (high density altitude) at the desired deviation from the international standard atmosphere (ΔISA) as well as cruise conditions. The ΔISA was set to +25 K for this retrofit application case.

Independent investigations were performed before the actual powertrain sensitivity studies, as ICCE was not directly coupled to BLADE but needed to be executed in advance. A fixed TMS configuration was derived and was not altered throughout the aircraft design process. The results of the aforementioned studies were then integrated into BLADE by means of general performance parameters, such as specific power or power density. After the first estimations on the expected waste heat of the hydrogen-electric system were obtained, the TMS was designed and calculated for a range of input parameters to derive the overall system behavior trends. A multipoint design for takeoff ambient conditions at ΔISA = +25 K, as well as designed cruise conditions, was carried out to ensure the correct sizing of the TMS for all expected conditions. The system was then optimized in terms of mass, drag, and power consumption according to reference (turboprop) aircraft sensitivities for an intermediate-to-high power fraction provided by the FC (e.g., 20%), resulting in waste-heat values of around Q = 350 kW to be handled by the TMS. For lower power fractions resulting in heat loads deviating from this optimization target, the error of the TMS calculation increased, but became smaller in absolute values, as the overall heat load was reduced. Therefore, this approach was deemed sufficiently accurate for the planned studies.

Furthermore, the heat rejection capability of the FC was varied between 20 K and 40 K by altering the inflow and outflow conditions of the FC coolant with respect to its operating temperature of 220 °C. This enabled the analysis of the effects on the HEX drag due to the energy (waste heat) injected into the airflow.

The final TMS architecture consisted of a diffusor leading to a compact ram air HEX. Succeeding the HEX, a nozzle tried to convert the injected heat energy into thrust (reduced drag). For hot day ground operations, a puller fan was installed in the flow direction behind the HEX, which in turn was provided with the waste heat by a pumped cooling liquid. Within the BLADE calculations, the TMS was sized according to two input variables: the waste heat of the FC and the waste heat of the electric components (PEs & EM) at each given

mission point. The electric component of waste heat was derived by the power throughput and the efficiencies of the components under the assumption that all losses are converted into heat, which can be discharged by the TMS (no radiation or convective cooling within the nacelle). The waste heat of the FC, derived from its efficiency-over-power characteristic at each mission point, was then added to the electric component of waste heat and formed the sizing requirement for the TMS. Note, that the power consumption of the TMS was dependent on the amount of waste heat to be discharged, which iteratively increased the power requirement of the FC. To control this, an additional parameter was introduced, referred to as the TMS power ratio, which is defined as the power required to operate the TMS as a fraction of the waste heat it has to handle.

The higher operating temperature of the HT-PEFC led to high TMS specific powers, thus leading to a smaller system size which could be integrated directly into the nacelle. This led to two independent cooling systems: one for each nacelle's FC system with each having one HEX on the side of the nacelle generating additional drag due to the nacelle surface-area increase and the HEX pressure loss. There were no additional wires or pipes required from outside of the nacelle, as the TMS power consumption was entirely covered by the FC.

Advanced technologies such as the pre-cooling of propulsion system components with the cryogenic hydrogen during refueling or using the hydrogen on board as a heat sink were neglected as the focus of the study was on a short-term technology level. A summary of the incorporated TMS design parameters with their respective values can be found in Table 2 in Section 2.2.5.

2.2.4. Liquid Hydrogen Tank & System

Compared to gaseous hydrogen, liquid hydrogen (LH_2) has a higher volumetric and gravimetric energy density and was therefore chosen as a storage state for the hydrogen required to fuel the HT-PEFCs. The cryogenic temperatures required to store the LH_2 come with several challenges such as a high power demand for the liquefaction before fueling the aircraft or comparably heavy tank systems. Nevertheless, the drawbacks of alternative storage methods are seen as less performant on aircraft level and are thus disregarded. Even though foam-insulated cryogenic tanks are cheaper and lighter, a vacuum tank design was chosen for its low thermal conductivity, and thus its boil-off rate [30].

The LH_2 tank was designed directly within the aircraft design loop of BLADE with the in-house developed OpenMDAO-based tool HyDRA (Hydrogen tank Design, Ramifications and Assessment, [30]). This tool considers various parameters such as the allowable boil-off rate, ambient conditions, venting pressure, material properties, and safety factors and sizes the tank according to the required LH_2 storage mass. Given the geometric constraints, a thermal design of the insulation layer. as well as the mechanical design of the structural layer, were performed following a simplified approach [31,32].

The LH2 tank was set up to have a constant outer diameter of 1.08 m between the end caps, as this was the maximum possible diameter that could be fitted at the 2-seat side of the cabin without interfering with the aisle space. The end caps formed round semi-spheres and thus had a length of 0.54 m each. The maximum allowable length for the entire tank was 3.81 m due to the maximum allowable number of seats to be removed (five rows).

Even though HyDRA may calculate and place multiple tanks simultaneously, it was decided to only include one single LH_2 tank, as the low power contribution of the FCs required no redundancy. Moreover, the tank was designed only for the design mission, as the diversion was planned to be flown by the combustion engines only (for more details refer to Section 2.4). Furthermore, the available space imposed a major challenge; for two tanks, two more end caps would decrease the maximum volume available for hydrogen storage.

As one of the main challenges during the conceptualization of a retrofit is to keep the center of gravity (CG) within its former certified bounds, the only feasible option for the placement of the LH_2 tank lies within the central fuselage section close to the wings.

A placement in the aft fuselage would shift the CG too far aft, even though the cargo compartment of the D328eco would be well suited for such an integration. Placing it into the central fuselage section is in direct conflict with the passenger cabin and leads to the compromise of placing it at the two-seat side of the cabin, contained in a separate fairing due to safety reasons. This placement blocked no emergency exits, as depicted in Figure 3, but required the removal of passenger (PAX) seats according to the required LH_2 mass and, thus, the tank size. Furthermore, this compromise allowed the tank to be placed close to the MTOM's CG, as this was imperative for retrofit studies.

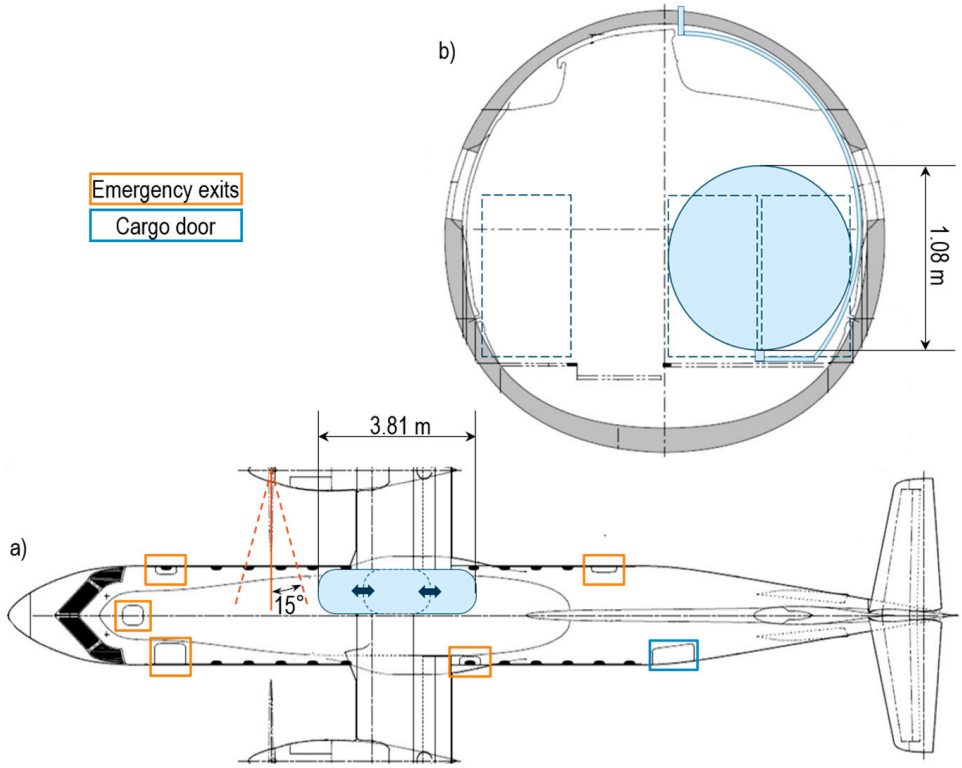

Figure 3. Schematic overview of LH_2 tank integration (blue) into the D328eco fuselage. (**a**) Top view incl. propeller blade-off angles, emergency exits, and cargo door; (**b**) Cross-section with seat location.

The hydrogen is transferred to the FCs via a vacuum-insulated piping system [33], which is calculated to start at the bottom of the tank, follows the curvature of the fuselage until it reaches the wing root and then splits into two pipes—one for each nacelle. A total pipe length of 14.85 m was calculated for the entire aircraft, including the nacelle internal routing. As the hydrogen flow rate required by the FCs under full load was comparably low due to the overall small power fraction on aircraft level, the piping was assumed to be for gaseous H_2 only. This led to the assumption that no additional power consumption was required to heat the H_2 within the pipes before entering the FCs, but around 15 kg of insulation mass for the protection of the aircraft structure against the cool pipes was added [34]. With an assumed mass of 2.0 kg/m for the filled tube and 5 kg of system installation mass, the entire mass for the H_2 transfer system was approximated to be around 50 kg. The LH_2 tank was placed inside a compartment to shield the cabin from any potential hazards related to it and its operation (refilling, leakages, etc.). Potentially, the ECS could provide a separate heating inflow into the LH_2 tank compartment to avoid the accumulation of excessive cool air, as well as condensation moisture.

Additionally, the venting would remove potential hydrogen accumulation and discharge it via a specific exhaust located at the top aft corner of the LH_2 tank compartment, thus, exiting the aircraft behind the wings trailing edge through the fuselage. Venting through the vertical tail plane (VTP) for maximum height above ground, as typically seen in clean-sheet designs, was disregarded as an installation through the existing structure

was deemed not feasible for a retrofit and would shift the focus of the studies away from the powertrain configuration options. As the H_2 quantities are comparably low, the chosen approach was considered to be adequately safe. The LH_2 tank compartment also serves as a barrier for the passengers in case of a major tank malfunction or tank rupture, with the same vent opening acting as pressure relief valves towards ambient conditions. This is especially important, as larger tanks approach the blade-off hazard angle of the propeller ($\pm 15°$ from the propeller plane, [35], see Figure 3). The mass of the LH_2 tank compartment walls was not taken into account, as it may be weighed against the removal of other furnishing parts as wall panels or window blinds. Nevertheless, it should be stated that the safety management for a cabin tank is far more critical than for an aft fuselage tank and would need further investigation.

2.2.5. Hybrid Powertrain Components

Due to changes in the powertrain, the nacelle volume needs to account for numerous additional systems. The nacelle surface was sized according to the actual volume of the incorporated systems with an additional oversizing factor of 5% to account for the reduced packaging efficiency of components.

For redundancy purposes, between the nacelles, there was a power cross-feed installed. This cross-feed enabled the transfer of electric power from one nacelle to the other in case of an FC system malfunction. The mass was assumed to be 5 kg/m, including all relevant safety switches and accessories. With a total cable length of 10.1 m, including 1.5 m routing within each nacelle, the entire mass of the power cross-feed was 50.55 kg.

The DCDC converter and DCAC inverter were resolved as two separate components within the powertrain assessment during the aircraft design loops but are referred to as power electronics (PEs) to simplify statements. They convert the power coming from the FC system to voltage levels and frequencies usable by the electric motor (EM). The incorporation of performance maps for these electric components was not deemed beneficial for the chosen model setup and did not align with the overall level of detail employed in other aspects of the design loop; hence, it was disregarded. This is valid assuming, that there were no significant EM efficiency changes between the design and off-design. Moreover, the negligible transmission distances between the respective components within the nacelle strongly reduce the impact of voltage-coupled performance maps. Therefore, the mentioned electric components were modeled based on specific power, efficiency, and power density without the assumption of large technological advancements for an EIS in 2035. Details can be found in Table 2 below.

A three-shaft gearbox is considered for this propulsion system, having one shaft for the turboshaft engine and one for the electric motor. The power of the two shafts is then combined and fed to the propeller. This concept allows for two different entry-shaft speeds, thus enabling each system to operate at its optimum. Furthermore, the separation enhances redundancy compared to an electric motor placed directly on the power shaft of the turboshaft engine. As this gearbox design differs from conventional configurations, the calculated GB mass was scaled by a factor of 1.2 and it then depended on the combined sea-level maximum power of the turboshaft and electric motor. The GB was expected to be air-cooled with no additional power consumption to be considered.

Between the EM and GB, as well as the TS and GB, shaft and bearing mechanical losses were considered as these were required for proper load bearing and vibration damping. A summary of the most important parameters is showcased in Table 2.

Table 2. Hybrid propulsion system component assumptions.

High-Temperature Polymer-Electrolyte FC	Value	Unit
Max. stack power	114	kW
Idle power	4.7	kW
Max. system efficiency	0.637	-

Table 2. *Cont.*

Power density	4.2	kW/L
Specific power	1.5	kW/kg
Operating temperature	493.15	K
Thermal management system		
Specific power [1]	5.0	kW(heat)/kg
Power density [1]	2.0	kW(heat)/L
Power ratio	0.08	-
Mechanical components		
Mechanical transmission efficiency	0.995	-
Gearbox transmission efficiency	0.985	-
Gearbox power density	80	kW/L
Gearbox mass factor	1.2	-
Electric components [2]		
Cable mass	5.0	kg/m
Power electronics efficiency	0.991	-
Power electronics specific power	15.6	kW/kg
Power electronics power density	20.4	kW/L
Electric motor efficiency	0.978	-
Electric motor specific power	19.1	kW/kg
Electric motor power density	35.1	kW/L

[1] Derived from BHL-internal, system-specific calculations. [2] From [36,37].

2.3. Study Setup

In this section, an elucidation of the study's setup is presented. The objective of this study is the conceptual design of a hydrogen-hybrid aircraft retrofit. In facilitating the comparative analysis and discussion regarding potential advantages conferred by innovative technologies, it is essential to incorporate both a reference aircraft as well as an EIS 2035 baseline aircraft. Given the adoption of a retrofit methodology, the assumption was made that no prospective advancements were applied to the aircraft aside from the integration of the novel propulsion system. Consequently, considerations pertaining to aerodynamic or structural innovations were excluded and there were no modifications to the subsystem, as these are already included in the engine deck in the form of fuel consumption (details see Section 2.2.1). Therefore, the contemplation of an EIS 2035 baseline aircraft became negligible, and only the reference aircraft was taken into account for comparisons to derivatives of the future hydrogen-hybrid aircraft retrofit in the ensuing studies.

In the course of these studies, aircraft modeling was conducted in the BLADE framework, which was introduced at the beginning of this chapter. More information on the sizing process can be found in [12]. The first step of the setup involved the meticulous calibration of the reference aircraft. To achieve this, all relevant data encompassing geometric attributes, mass distributions, and CG locations were derived in close cooperation with DA. Employing this dataset as the input, the aerodynamics of the aircraft model underwent calibration to ensure congruence with a predefined payload range diagram, thereby aligning the resulting mission performance data with the specified criteria.

The next step in the study setup involved the conversion of the calibrated reference aircraft into a hydrogen-hybrid configuration. Given that the hybridization is executed as a retrofit, the geometric and mass characteristics remained invariant, with alterations permitted exclusively with respect to the propulsion system. The sizing of the propulsion system was orchestrated within the iterative aircraft design loop. This iterative process entailed the adjustment of the design top of climb (TOC) thrust to meet the stringent criteria of both takeoff field length (TOFL) and time to climb (TTC). The sizing of the powertrain was contingent upon the most restrictive criterion among them, which was dynamic and could change throughout successive iterations of the sizing process.

As the turboprop engines of the reference aircraft are capable of using pure SAF alongside conventional Jet A-1 kerosene, the retrofit studies aimed for the best-case scenario of burning pure SAF. To enhance data transparency, SAF from 100% hydrotreated esters and fatty acids (HEFA) was used instead of a more typical blend. Both fuels have a value range for density and lower heating value (LHV), but it was decided to proceed with the following values according to [38]: a density of 757.0 kg/m^3 (Jet A-1: 790–810 kg/m^3) and an LHV of 44.1 MJ/kg (Jet A-1: 43.2–43.3 MJ/kg). The increased fuel volume due to the reduced density of the SAF had no impact on the retrofit design and the use of the wing integral tanks, as the fuel required, was decreased depending on the power fraction of the FC.

As the aircraft embodied a dual-fuel hybrid configuration, it became imperative to account for the changes in fuel mass and the LH_2 tank. Commencing with a computed SAF mass for the reference aircraft, the requisite SAF and LH_2 masses were derived through the utilization of their LHVs and a predefined power split, expanded in the following Section 2.4. This facilitated suitable initial conditions for the aircraft design process and mitigated the risk of divergence. Subsequently, during each aircraft iteration, the SAF and LH_2 masses were computed utilizing the engine deck and fuel cell model, respectively, based on the mission performance data, and the LH_2 tank dimensions and mass were calculated using HyDRA.

As the incorporation of supplementary propulsion system components inevitably leads to a higher total propulsion system mass while the MTOM must remain invariant, a reduction in payload mass was necessitated in exchange. The requisite reduction of payload mass was dynamically incremented to offset the augmented mass contributions emanating from the propulsion system, tanks, and fuels, ensuring an alignment with the prescribed MTOM.

Given the stipulated minimum requirements for the retrofit to still result in a reasonable product, a further constraint pertaining to the dimensions and placement of the LH_2 tank was introduced. Since the tank was positioned inside the fuselage, the payload had to be removed. The tank width was predetermined according to cabin constraints while the length was adjusted to match the required volume with the necessary LH_2 mass. The tank's length exerted influence on the passenger count, which was adjusted according to the remaining available seats. In compliance with the requirement of a minimum capacity of at least 30 PAX, an upper limit on the maximum tank's length was imposed. It is imperative to emphasize that the payload constituted a composite of passengers and cargo. Consequently, its reduction was not executed discretely through the removal of a specific count of passengers but changed continuously on a per-kilogram basis, adhering to the constraints imposed by the maximum tank length.

The sizing of the propulsion system and masses were iterated during the aircraft design loop until all values were converged and the sizing goals were met.

2.4. Hybridization Strategy

Considering the hybrid powertrain described in Section 1.2, and the sizing process outlined in Section 2.3, an additional parameter needed to be specified to control the power allocation between the TS and the FC. This parameter is referred to as the power split (S_P) and is defined in Equation (2):

$$S_P\,[\text{-}] = P_{FC}/(P_{TS} + P_{FC}), \tag{2}$$

with

$$P_{FC}\,[\text{W}] = P_{A/C} * S_P/\eta_{Total} \tag{3}$$

as well as

$$P_{TS}\,[\text{W}] = P_{A/C} * (1 - S_P)/(\eta_{GB} * \eta_{MECH}) + P_{Subsystems} \tag{4}$$

and

$$\eta_{Total}\,[\text{-}] = \eta_{GB} * \eta_{MECH} * \eta_{EM} * \eta_{PE}{}^2 \tag{5}$$

with the PE efficiency being counted twice to account for both the converter and inverter. Consequently, a power split definition was required for the design point and each mission flight point.

In this study, each aircraft mission was modeled as a collection of segments, each having different specifications regarding the powertrain operation. Throughout any cruise and loiter segments, the powertrain was configured to meet the aircraft's thrust requirement, thus a power split needed to be defined. However, during any takeoff and climb segments, the powertrain was engaged at its maximum available power, and during any descent and landing segments, it operated at idle. Therefore, no power split specification was required. This led to a variable power split during these segments, dependent on the power lapse of each system with altitude due to the decrease in air density. Based on the models detailed in Sections 2.2.1 and 2.2.2, the FC power lapse was less significant than that of the TS, leading to an increased power split with altitude.

Moreover, the incorporation of FCs yielded emission reductions mainly during the cruise, leading to the deliberate exclusion of FC operation during the diversion. This strategic decision was reinforced by the potential consequence of increased hydrogen usage, which could lead to tank lengths exceeding the predefined limits.

An additional strategy was considered, for which the fuel cell was operated at its maximum power and the turboshaft was de-rated to match a prescribed power split for all segments. Since the takeoff and climb segments were used for the powertrain sizing, see Section 2.3, this de-rating would result in an oversizing of the turboshaft and its available power would not be fully utilized. For this reason, such a strategy was not further explored.

3. Results

This chapter outlines the main findings of the executed studies based on the predefined methods and models. Initial preparatory studies are conducted to establish the baseline parameters that every other study is compared to, succeeded by a series of parameter studies aiming at exploring various effects on specific areas of interest.

3.1. Preparatory Studies

The following preparatory investigations aim to determine a range of baseline values for parameters of interest so that an appropriate comparison can be made in the subsequent parameter studies. These investigations include the derivation of a baseline hydrogen-hybrid aircraft along with its hybrid-specific characteristics, as well as an independent investigation into the TMS requirements and their corresponding specific power sensitivities.

3.1.1. Baseline Aircraft

Based on the aforementioned study setup, models, methods, and hybridization strategy detailed in Section 2, a baseline hydrogen-hybrid configuration was derived. A design power split of 0.2 was chosen following a preliminary design space assessment, and concurrently, the cruise power split was set at the same level to prevent exceeding the limits of either the TS or FC maximum available powers. A comparison between the reference and baseline aircraft is presented in Table 3. As per TLAR specification, the MTOM, design range, and TOFL were kept constant.

As shown in Table 3, the propulsion system mass experienced a notable increase of 749 kg (34.5%), and with the incorporation of the LH_2 tank, an overall operational empty mass (OEM) increment of 848.7 kg (8.4%) was determined. Although this would intuitively translate to an equivalent payload mass decrement, a disparity was found, which was reconciled by considering the reduced SAF usage and the added LH_2 mass. This arose from an SAF reduction of 213.3 kg (12.9%) and the inclusion of LH_2 with a mass of 63.5 kg, counteracting the payload mass decrease. Additionally, a difference of -0.5% in the cruise lift-to-drag ratio was determined, mainly attributed to the variation in the cruise aircraft mass and CG shift due to the LH_2 tank positioning and powertrain mass difference.

Table 3. Comparison of reference aircraft against baseline hydrogen-hybrid configuration.

Variable [Unit]	Reference	Baseline	Δ [%]
Operational empty mass [kg]	10,150.0	10,998.7	+8.4
Payload mass [kg]	3880.0	3178.7	−18.1
Propulsion system mass [kg]	2173.6	2922.5	+34.5
Hydrogen tank mass [kg]	0.0	79.7	-
SAF mass [kg]	1650.0	1436.7	−12.9
Hydrogen mass [kg]	0.0	63.5	-
Cruise Lift-to-Drag Ratio [-]	13.2	13.1	−0.5

3.1.2. Thermal Management System Assessment

As expected, the incorporation of HT-PEFCs strongly facilitated the overall FC system integration into the aircraft, as the elevated operating temperature compared to conventional low-temperature (LT-)PEFCs allowed for a far smaller and lighter heat exchanger design. This reduced the external component size, leading to less HEX pressure loss as well as HEX fairing drag. Specifics on the TMS design can be found in Section 2.2.3.

Detailed studies were carried out to assess the performance characteristics of the thermal management system for varying heat loads, and thus propulsion system power split arrangements, as well as two different heat rejection capabilities of the FC-TMS combination. As the spread between FC coolant inlet to outlet temperature was increased from 20 K to 40 K, the nozzle behind the HEX was able to convert the increased energy input, thus, expanding air into more thrust per unit time and reducing the overall TMS drag. The larger spread of the coolant was represented by the lower coolant inlet temperature ($T_{2,h}$) (Figure 4) as it was compared to the FC operating temperature of 493 K. The aforementioned change in drag, the trends for the FC power consumption, the mass, and the HEX volume for the entire system can be found in Figure 4.

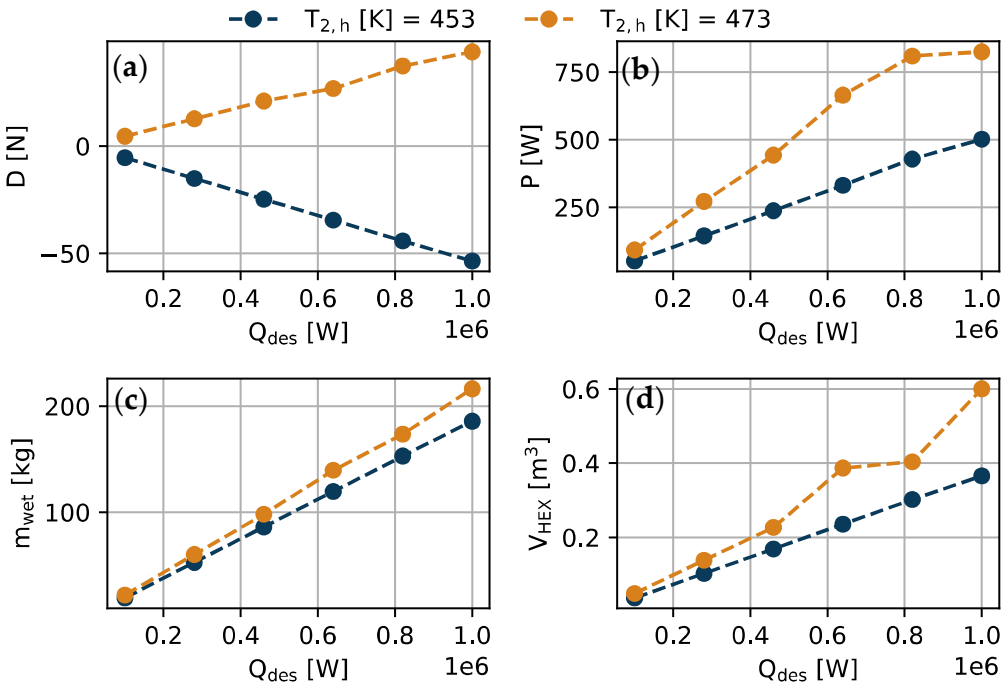

Figure 4. The plot of the TMS design results for a rise in coolant temperature of 20 K (orange) and 40 K (blue); (**a**) TMS drag overheat load; (**b**) TMS power required to overheat load; (**c**) TMS mass incl. fluids overheat load; (**d**) HEX volume overheat load.

The increase in operating temperature from around 80 °C of a conventional PEFC to the assumed 220 °C (493 K) of the HT-PEFC comes with several advantages if FC-internal challenges are neglected. The size and, thus mass decrease, of the HEX resulted in very

high TMS specific-power values of 4.69 to 5.31 kW(heat)/kg (see Table 4). Therefore, for most of the presented studies, an averaged TMS specific power of 5.0 kW(heat)/kg was assumed. The results of the TMS specific power variation, quantifying the influence of the TMS specific power on the aircraft level, can be found in Section 3.2.1. As shown in Table 4 below, the increase in the FC heat rejection capability allowed for a smaller heat exchanger volume, which in turn reduced the HEX-internal drag due to a reduced flow-path length and, therefore, the power consumption of the TMS pumps. The heat rejection capability of the FC purely depends on the internal construction of the FC with its cooling channels and temperature dependence of the chemical processes. As a detailed FC, design is not part of these studies, the presented results remain a theoretical assessment, which might be applied to other detailed FC studies. On aircraft level, the reduced HEX size will also decrease the wetted area of the nacelle, which in turn reduces the aircraft surface drag.

Table 4. Results of the TMS design optimization for a design heat load of Q = 350 kW.

FC Heat Rejection Capability [K]	**40**	**20**
Drag [N]	−19	16
Power [W]	199	353
Mass (wet) [kg] [1]	66	75
Volume (HEX) [L]	129	171
TMS specific power [kW(heat)/kg]	5.31	4.69
TMS power density [kW(heat)/L]	2.71	2.05

[1] Mass excluding pumps due to methodical reasons.

Note, that the numbers presented in Table 4 are only valid for a TMS design heat load of 350 kW and that the lower 2.0 kW(heat)/L TMS power density was used for the remaining studies. The latter has a direct impact on the aircraft performance, as the power density directly relates to the volume of the TMS, and therefore nacelle size, as the HEX fairing is incorporated into the nacelle wetted surface due to its installation at the nacelle side.

3.2. Parameter Studies

The following investigations aim to determine the influence of varying several powertrain components' technology assumptions, such as specific power and the various effects of fuel cell oversizing strategies. Furthermore, a set of conservative technology-level parameters is defined, upon which a minimum viable product is derived and analyzed. The baseline derived in Section 3.1.1 serves as a basis for comparison.

Note that for all subsequent studies, the hydrogen tank length does not exceed the imposed limitation for any configuration and the turboshaft engine is able to provide the required power to result in a diversion performance comparable to the baseline aircraft, during which no fuel cell power is drawn. However, the payload mass budget is exceeded for some of the edge cases of the studies, signifying that the specific power of the powertrain components and the hydrogen tank gravimetric index are the most influential parameters.

3.2.1. Specific Power Variations

Given the inherent uncertainties associated with the precise prediction of the FC system performance characteristics in 2035, particularly concerning the power-to-weight ratio, a series of parameter studies was undertaken to analyze the impact of the specific power of the FC on the aircraft characteristics. The same uncertainty accounts for the TMS, being the reason for a second specific power variation. This investigation comprised two distinct studies, varying the FC and TMS specific powers independently. It is important to note that all other stipulated requirements and parameters were held constant throughout these analyses. As explained in Section 2.3, the payload mass was varied to keep the MTOM constant.

The investigation of the specific power of the TMS showed that for values of 1.0 and 2.0, the minimum payload mass was surpassed, as the increased propulsion system mass could not be compensated. Therefore, the MTOM would have to increase, which was why these studies were deemed invalid. This underlines the strong impact of the TMS design in conjunction with the operating temperature of the FC.

As expected, in both studies, the FC specific power variation and the TMS specific power variation delivered very similar effects on an aircraft level. Next to the actual results, this was also a valuable crosscheck of the accuracy of the implemented models, as the effects on aircraft level were closely linked. Through the change of the specific power values, the mass of the propulsion system was changing, whereby a higher specific power was leading to a lower propulsion system mass. As previously delineated, the adjustment in payload mass was implemented to offset the reduction of the propulsion system mass, as visually represented in Figure 5.

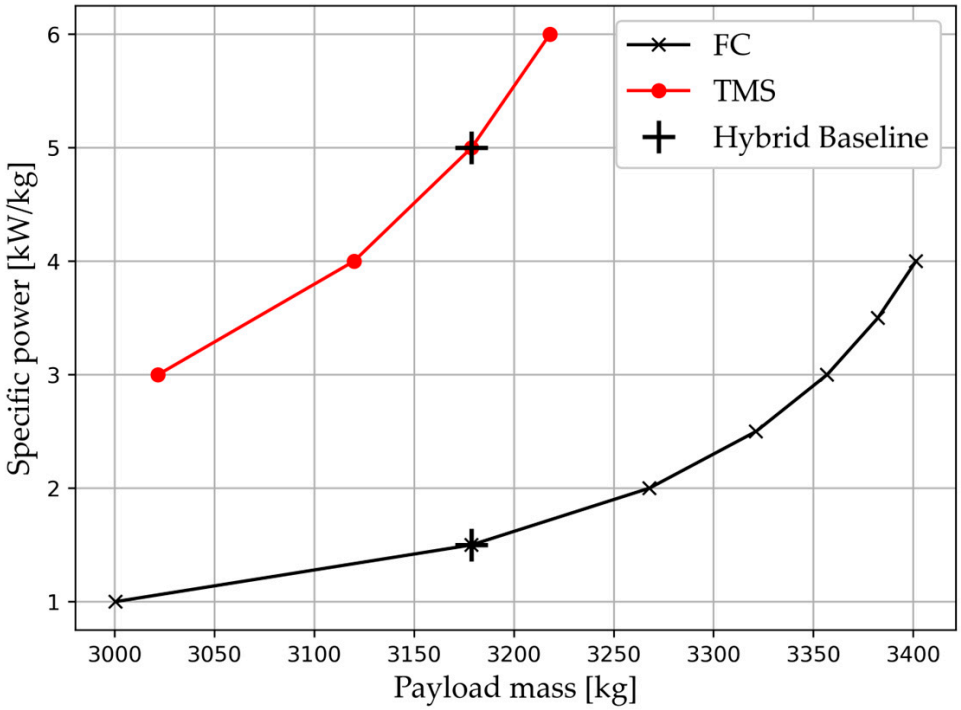

Figure 5. Variation of payload mass with FC and TMS specific powers.

Doubling the specific power (from 2.0 to 4.0 for the FC and from 3.0 to 6.0 for the TMS) led to a reduction of the propulsion system mass of about 134 kg for the FC and 196 kg for the TMS. This discernible disparity underscored the superior influence of the TMS's specific power on the propulsion system mass as compared to the specific power of the FC. It is imperative to note that these observations only hold within the specified ranges, given the non-linearity inherent in the depicted curves. Yet, as the power density of the TMS was lower compared to the FC, the additional volume increased the nacelle size and therefore made the drag stronger. Moreover, as the nacelles were not located at the CG, FC and TMS specific power changes led to a CG shift and therefore trim drag changes with the accompanying snowball effects.

3.2.2. Fuel Cell Oversizing

To investigate the influence of the propulsion system mass and efficiency on the aircraft performance characteristics, an additional parameter was introduced in the powertrain design point definition, referred to as the fuel cell design factor (F_D). This factor can be used to increase the fuel cell system design power for a given design point in order to enlarge the margin between the required and available power at each flight point.

However, any additional power that is present due to this scaling is not made available during the powertrain operation. Hence, while opting for an oversized fuel cell system leads to a heavier propulsion system, the power demand at any given flight point is a reduced fraction of its maximum power compared to an unscaled variant, thereby yielding improved efficiency. This benefit is present only if the power requirements are not scaled with the propulsion system mass. As detailed in Section 2.3, a payload increment was implemented to uphold a designated MTOM, thus any rises in the mass of the propulsion system would be offset by the presence of this increment.

To quantify the aforementioned effects, a parameter study with a varying F_D was performed. The F_D was increased until the minimum payload mass limit was reached. The results of this study are presented in Table A1 and Figure 6. Note that an F_D of 1.5 was also investigated, however, the resulting aircraft payload mass was below the predefined limit and, therefore, an F_D of 1.4 was the highest viable case examined. Consolidating all relevant data from Table A1, along with the cruise performance characteristics corresponding to this case, it was shown that fuel cell oversizing could lead to a 5.1% decrease in hydrogen mass flow during the cruise. The balancing of payload and propulsion system masses needed to maintain the MTOM culminated in a CG shift of 0.3% towards the aircraft nose, thus increasing drag by 0.3% to ensure trimmed flight. This caused an equivalent thrust/power requirement raise, which produced a 0.23% increase in SAF mass. Despite that, the collective effect of hydrogen mass flow reduction and elevated thrust demand still resulted in a decrease in hydrogen mass of 7.7%.

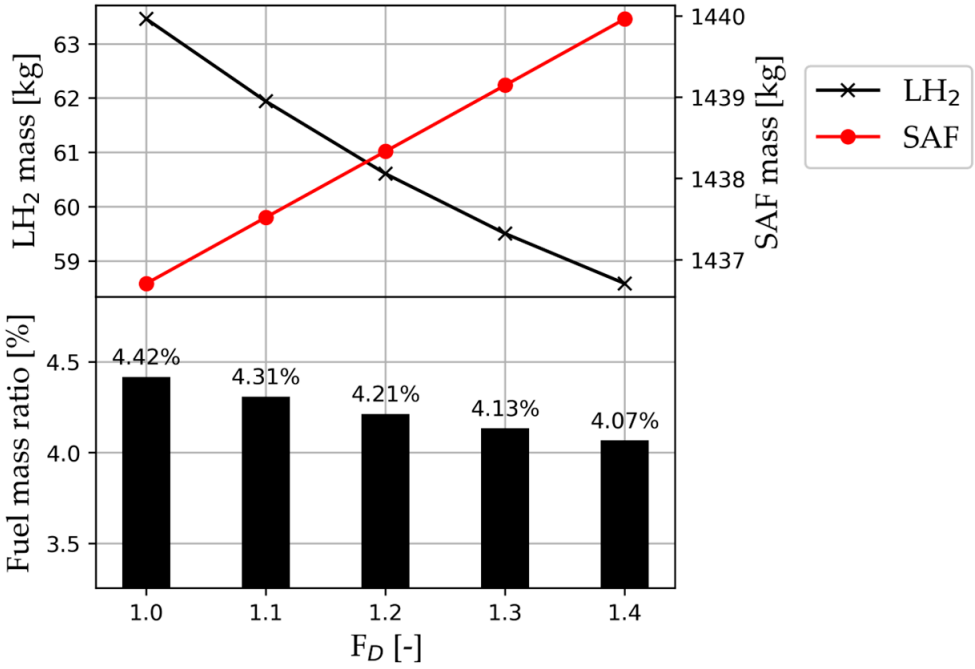

Figure 6. Variation of fuel masses with F_D.

All cases in this study were analyzed with a fixed cruise power split specification of 0.2, always increasing overall SAF consumption as the fuel cell was oversized. To mitigate this effect, an additional parameter study was performed, where the cruise power split specification was varied until the maximum available fuel cell power was used during the cruise. For all subsequent cases, the highest viable F_D of 1.4 was employed. The results of this study are presented in Table A2 and Figure 7.

For the specified F_D, a maximum allowable cruise power split of 0.28 was reached, which culminated in a hydrogen mass increase of 32.4% (20.6kg) and a SAF mass decrease of 3.63% (52.1kg). This study aimed to identify a variant that minimized SAF consumption and in turn emissions. Two metrics were utilized, namely the actual SAF mass consumed and the SAF mass to payload mass ratio. Figure 8 illustrates the variation of the oversizing

factor and cruise power split against both of these metrics. It is evident that if the total emissions were the main objective to be minimized, then the fuel cell oversizing and cruise power split had to be maximized. On the other hand, if the emissions per passenger were required to be minimized, employing a fuel cell oversizing would result in diminishing returns regardless of any additional cruise power split increase.

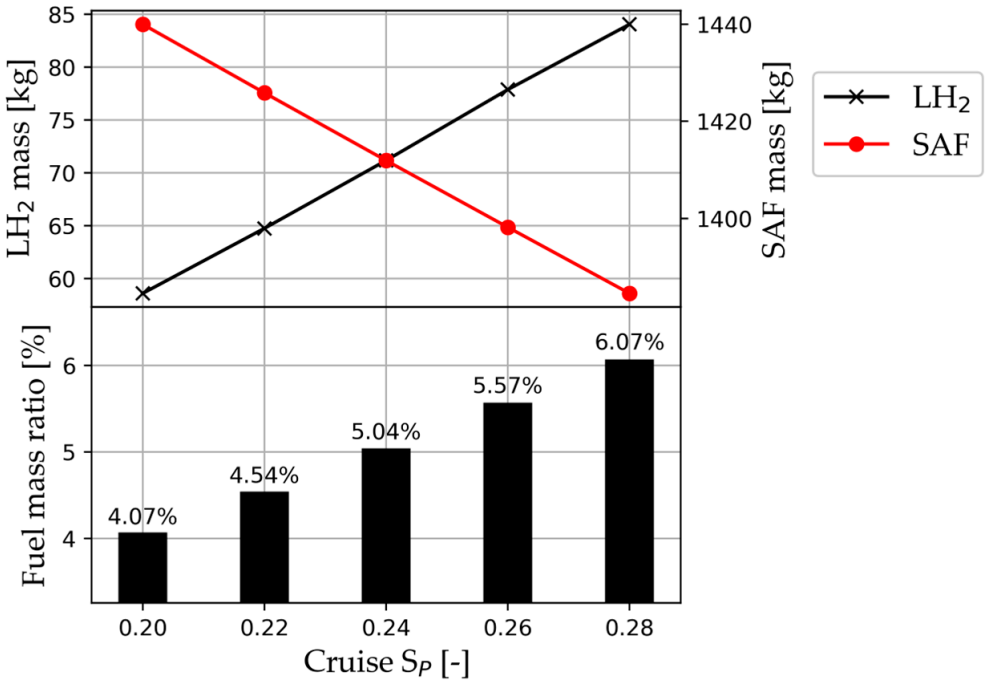

Figure 7. Variation of fuel masses with cruise S_P.

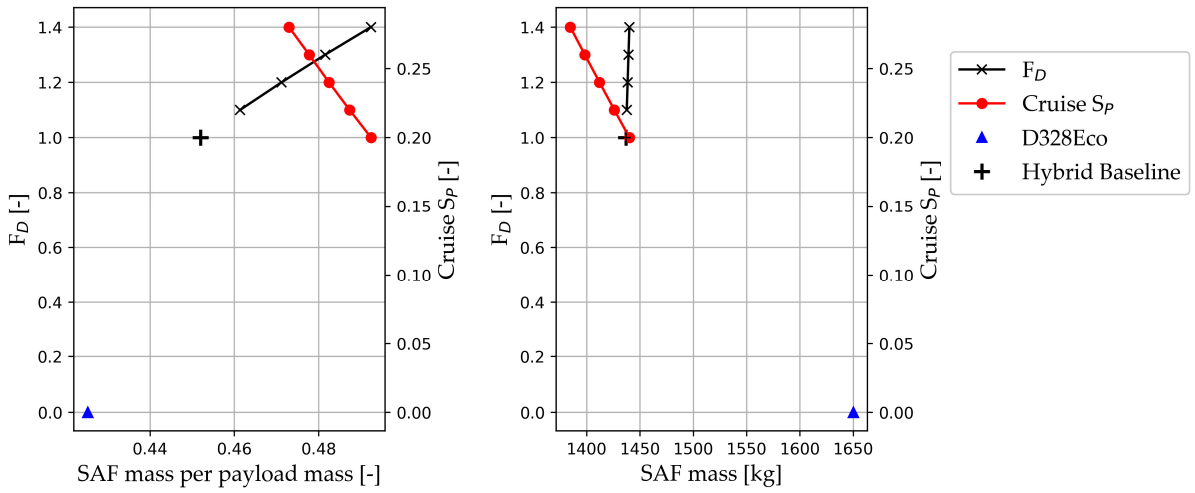

Figure 8. Variation of SAF mass per payload mass (**left**) and SAF mass (**right**) with F_D and cruise S_P.

3.2.3. Minimum Viable Product

In this study, design parameter specifications for a minimum viable product (MVP) were investigated, scrutinizing the implications within a worst-case scenario for the year 2035 aircraft design. The aim of this study was to derive a limiting case for a retrofit based on conservative hybrid powertrain assumptions. Given these changes, the largest possible power split was applied to maximize the hydrogen power share and reduce the fuel consumption of the combustion engines and, thus, emissions.

Accordingly, major requirements were set to their minimum values. Specifically, the payload mass was established at the minimum stipulated count of passengers, constituting 30 PAX and resulting in a payload mass of 2910 kg, while maintaining the MTOM at a constant level. The minimum range requirement was set at 200 NM, thus reducing the overall energy-carrier mass on board, which was necessary to accommodate the installation of a heavier propulsion system. In contrast to the HT-PEFC introduced in Section 2.2.2, the powertrain assumptions were adopted to a low-temperature PEFC with its major drawbacks associated with the TMS. Furthermore, the gravimetric index of the LH_2 tank was fixed to a rather low value of 30% and not calculated based on the hydrogen mass, as in the other studies. Lastly, the TMS specific power was reduced to 2.0 kW(heat)/kg to account for the strongly reduced temperature spread of waste heat and ambient air.

The aircraft design loop was re-executed with these refined input parameters, yielding the values presented in Table 5. Using the above-mentioned assumptions, a design power split of just under 30% was achievable. Notably, the TMS mass experienced a substantial increase, nearly quadrupling for the MVP in comparison to the baseline. While there was a decrease in the masses of hydrogen (−52.0%) and SAF (−41.6%), the masses of the propulsion system and fuel cell increased by 31.6% and 57.5%, respectively. Due to the low total hydrogen mass, the LH_2 tank length was far from its length limit even though the maximum of 10 PAX needed to be removed due to mass constraints. This observation showed that, if combined with the payload and despite a pronounced augmentation in the propulsion system mass and the reduction of the payload to its lower threshold, the SAF consumption per kilogram of payload was only 63.8% of the baseline. Nevertheless, this came with the drawback of a major range and payload reduction.

Table 5. Comparison of Baseline and minimum viable product for selected parameters.

Variable [Unit]	Baseline	MVP	Δ [%]
Payload Mass [kg]	3178.7	2910.0	−8.5
Hydrogen Mass [kg]	63.5	30.5	−52.0
Hydrogen tank mass [kg]	79.7	74.1	−7.0
SAF Mass [kg]	1436.7	839.0	−41.6
Propulsion System Mass [kg]	2922.5	3846.5	+31.6
Fuel Cell Mass [kg]	178.7	281.4	+57.5
TMS Mass [kg]	119.7	471.4	+293.8
Power Split [-]	0.2	0.298	+49.0
FC Specific Power [kW/kg]	1.5	1.5	0.0
TMS Specific Power [kW/kg]	5.0	2.0	−60.0
Block range [NM]	580	200	−65.6
SAF mass/Payload mass [-]	0.45	0.29	−36.2
SAF mass/(Payload mass ∗ Range) [1/NM]	7.79×10^{-4}	14.42×10^{-4}	+85.0

It was furthermore investigated if the utilization of the FC during diversion climb could reduce the overall propulsion system and energy carrier mass, but no advantage was found. The TS engine size and LH_2 tank mass effects showed no noticeable impact for increasing power splits and were therefore disregarded in terms of diversion setup.

4. Discussion

Given the target to minimize development time and risks, as well as infrastructure changes, retrofitting existing aircraft, such as the D328eco used in the presented study, might be a valid option. It can be concluded that for a carefully selected set of assumptions, a dual-fuel hydrogen-hybrid retrofit of the D328eco aircraft is feasible. Even though a reduction in the passenger number is inevitable, an integration of hydrogen FCs will reduce emissions, especially in the most climate-relevant section of the flight—the cruise.

The hybrid baseline with its power split of 0.2 led to a SAF reduction of 12.9% while the payload was reduced by 18.1% to counteract the increase in propulsion system mass and the addition of the LH_2 tank mass. Moreover, changes in the CG location, due to the

placement of propulsion system components, decreased the lift-to-drag ratio by 0.5% due to an increase in trim drag.

These two effects summarize the challenges of retrofit designs well; the limited component-placement flexibility of the propulsion system due to the enlarged system and the aircraft modification restrictions induce negative properties in terms of CG location and mass. Apart from a series of requirements, it must especially be ensured that the wing-mounted mass is not exceeded, since for this type of retrofit the propulsion system mass is the focal point.

Specific power variations revealed that the TMS has a greater lever in terms of mass compared to the FC system. The mass increase resulting from halving the FC specific power was 68.4% of the mass increase arising from the halving of the TMS specific power. Additionally, the lower power density of the TMS compared to the FC resulted in raised drag values, thus leading to higher thrust requirements and in turn a larger and heavier propulsion system.

Independent FC oversizing reduced hydrogen consumption by 7.7% with no significant effects on SAF, even though the increase in propulsion system mass needed to be counterbalanced by a decrease in payload mass. This underlines that oversizing is generally beneficial for longer flight distances, as the hydrogen mass savings due to the efficiency increase during cruise might outweigh the FC system mass increase. In case a maximum SAF reduction is aimed for, the oversizing allows for higher cruise power splits. For a FC oversizing of 40%, the power split could be increased to 0.28 (baseline: 0.2), resulting in a 32.4% increase in hydrogen required with a simultaneous reduction in SAF by 3.6%. Based on these results, FC oversizing and cruise power split maximizing was found to be the most successful approach investigated to minimize total SAF mass and, therefore, emissions. However, to minimize SAF per passenger, used as an alternative metric for comparison against the reference aircraft, no oversizing is deemed beneficial.

The studies were completed by investigating the lower limit of the powertrain assumptions to derive a minimum viable product incorporating a low-temperature PEFC and coupled low-performance assumptions. For a set of minimum requirements, the MVP achieved a reduction of 63.8% of SAF consumed per PAX compared to the hybrid baseline, while maximizing the power split, reaching a value of 0.298. Based on these results, the development potential of a D328eco retrofit could be judged while keeping the HT-PEFC studies in mind.

A key enabler for the presented retrofit is the FC design choice in conjunction with the TMS. Due to the large share of the mission requiring constant FC power, an aerospace-tailored FC design should differ from automotive applications in contrast to the chosen reference FC to maximize performance. Particularly, as high temperatures greatly enhance overall system performance, specific HT-PEFC designs should become the focal point of future developments. It may be expected that an aerospace-specific FC design might lead to more favorable characteristics, as costs are less relevant than in the automotive sector and different requirements are put into place (load characteristics, cycle number, system size, and mass, drastic changes of ambient conditions, etc.). Progress was claimed in this regard [39], but needs to be verified in actual applications.

The combination of the compressor with the environmental control system (ECS) would most probably be possible, as the ECS unit of a D328eco is in the frontal wing root above the cabin and additional space could be allocated. Furthermore, this would place it between the nacelles and allow for a simpler distribution of the compressed air. The drawbacks arising from this modification include the deterioration of redundancy, the additional piping length requirements, and the increased system cost due to complexity.

The TMS setup is directly coupled with the FC system performance. Depending on the requirements placed on the TMS design it may have a large lever on the overall aircraft performance as outlined in Section 3.1.2. Therefore, more advanced systems or altered operational strategies, compared to the typical compact HEX used for the presented studies, could yield superior TMS performance. An example of an alternative operational strategy

could be the use of the FC on cruise only, strongly increasing the lowest temperature spread due to the low ambient temperatures during the cruise. Yet, this comes with strong changes in the overall operational concept and would prevent emission-free airport operations on FC power only. Note that the TS engine would be required to still be operated, though at idle, to enable sufficient warm-up time. Furthermore, the propeller slipstream was not taken into account for the TMS design, underlining the rather conservative TMS design approach.

The heat rejection capability of the FC was found to have a major impact on the TMS performance. Therefore, it is a fundamental aspect to be considered for future aerospace-tailored FC designs. This is closely coupled to the properties and flow velocity of the cooling liquid chosen. Using the LH_2 as a heat sink, or to pre-cool e.g., electric systems, could be an option but was dismissed due to the model setup and uncertainties regarding technological readiness. A single TMS serving both nacelles could potentially be coupled with the ECS but would make a true retrofit less feasible, as more system changes to the baseline aircraft would be required.

As the LH_2 tank size is never limiting according to the assumptions chosen for the presented studies, the redundancy and hazard impact could be improved by incorporating two separate tanks, even though this comes with a mass penalty. This, in turn, prompts the question of whether identical or varying sizes and, consequently, mass distributions should be considered. In addition, the presence of multiple tanks also allows for various de-fueling strategies which can be tailored to optimize the CG shift during operation. Tank configurations with total lengths that result in maximizing the space utilization arising from seat row removal should be preferred, as these should lead to higher removed payload to LH_2 mass ratios. Furthermore, sloshing could be an additional consideration for longer tanks giving rise to a new set of aspects that should be investigated; however, this was not investigated with the current model setup.

On overall aircraft level, further modifications that were not part of the presented studies could be considered while keeping the retrofit requirements in place. If mass savings can be expected, specific subsystems could be electrified or interactions could be considered, such as using parts of the waste heat for wing anti-icing. Nevertheless, during the conceptualization of a retrofit, the overall costs play a major role and may outweigh investments in too complicated/expensive modifications, differentiating a retrofit, to a certain degree, from clean-sheet designs.

Finally, the aircraft size selected for a retrofit is of considerable importance, as trades between the cost of the modifications, design range of the retrofit, and propulsion system mass fraction vary massively between the different aircraft types. Regional aircraft may act as an enabler for the first hydrogen-hybrid retrofit concepts, as they commonly operate on less congested routes in remote regions, where there are few transport alternatives (e.g., Scandinavia, Canary Islands, etc.), but no long distances need to be covered. These shorter-range missions require lower total energy carrier quantities on board and have a reduced payload demand, rendering them ideal candidates for the integration of presently less power-dense propulsion systems.

It should be noted that retrofit considerations are a function of a multitude of requirements, with economic considerations commonly prevailing. The planned type of operation and especially the availability of hydrogen at relevant airports, including the refueling infrastructure, are of utmost importance for the realization of the discussed concepts and should therefore always be analyzed in parallel.

5. Conclusions

Various sensitivity studies were carried out on a dual-fuel hydrogen-hybrid regional aircraft retrofit based on the D328eco featuring a parallel-hybrid powertrain incorporating TS engines and HT-PEFCs as well as an LH_2 tank located inside the passenger cabin.

The hybrid baseline with its power split of 0.2 led to a SAF reduction of 12.9% while the payload was reduced by 18.1% to counteract the increase in propulsion system mass and the addition of the LH_2 tank mass. Specific power variations of FC and TMS revealed

that the TMS has a greater lever in terms of mass. Additionally, the lower power density of the TMS compared to the FC resulted in raised drag values, thus leading to higher thrust requirements and in turn a larger and heavier propulsion system. Independent FC oversizing reduced hydrogen consumption by 7.7% with no significant effects on SAF, even though the increase in propulsion system mass needed to be counterbalanced by a decrease in payload mass.

The studies were concluded by investigating the conservative, lower limit of the powertrain assumptions to derive a minimum viable product incorporating a low-temperature PEFC. For a minimum of 200 NM (baseline: 580 NM) and 30 PAX, the MVP achieved a reduction to 63.8% of SAF consumed per PAX compared to the baseline while maximizing the power split to 0.298. Nevertheless, on the other hand, this came with a significant 85% increase in SAF mass per PAX per NM.

As this article focuses on the setup of the reference and retrofit aircraft, as well as on the sensitivity studies for a range of powertrain parameters, a deeper analysis of the limiting cases and a refinement of the studies remain open. Future work should consider operating the FC during diversion since this might lead to enhancements in the TS-FC combined performance and possibly allow for higher achievable power splits. In direct dependency to the diversion is the use of two LH_2 tanks for redundancy. Moreover, for a given design, the typical mission should be analyzed to gain an understanding of the in-service performance of the retrofit, enabling an independent segment-wise power allocation optimization. Finally, to compare the reference aircraft against its hybrid evolution from an emissions standpoint, the typical mission aircraft characteristics have to be derived and paired with a corresponding fleet model, such that the overall environmental impact is appropriately considered.

Author Contributions: Conceptualization, methodology, software, validation, investigation, and writing of all aspects of the research except for Section 2.1, Section 2.2.1, Section 2.3, Section 2.4, Section 3.1.1, and Section 3.2.2, U.C.J.R.; methodology, software, validation, and writing of before excepted sections, A.L. & P.E.; visualization, A.L. and U.C.J.R.; project administration and funding acquisition, U.C.J.R.; supervision, M.H. All authors have read and agreed to the published version of the manuscript.

Funding: This research and the APC were funded by the German Federal Ministry for Economic Affairs and Climate Action under the German Aviation Research Program (LuFo) called VI-2, grant number 20M2109H (project 328H2-FC).

Data Availability Statement: Data are contained within the article.

Acknowledgments: We would like to thank our partners in the 328H2-FC project and especially Michael Shamiyeh from Deutsche Aircraft for the continued support and fruitful discussions. Furthermore, we would also like to thank Hagen Kellermann for his contributions to the TMS analysis as well as the Visionary Aircraft Concepts team at Bauhaus Luftfahrt for their dedicated work on BLADE and the inspiring discussions.

Conflicts of Interest: All authors were employed by Bauhaus Luftfahrt e. V. They declare that the research was conducted in the absence of any commercial or financial relationships that could be construed as a potential conflict of interest.

Nomenclature

328H2-FC	Project name
AC	Alternating current
BLADE	Bauhaus Luftfahrt Aircraft Design Environment
BoP	Balance of plant
CG	Center of gravity
DA	Deutsche Aircraft GmbH
DC	Direct current
ECS	Environmental control system

EM	Electric Motor
ICCE	Innovative Cooling Concept Environment
FC	Fuel cell
F_D	Fuel cell Design factor
FL	Flight level
GB	Gearbox
HEX	Heat exchanger
HyDRA	Hydrogen tank Design, Ramifications and Assessment
ISA	International standard atmosphere
HT-PEFC	High-temperature polymer-electrolyte fuel cell
LH_2	Liquid hydrogen
LHV	Lower heating value
MECH	Mechanical
MTOM	Maximum takeoff mass
MVP	Minimum viable product
NM	Nautical miles
OEM	Operational empty mass
P	Power
PAX	Passengers
PE	Power electronics
SAF	Sustainable aviation fuel
S_P	Power Split
TMS	Thermal management system
TOC	Top of climb
TOFL	Takeoff field length
TS	Turboshaft
TTC	Time to climb

Appendix A

Table A1. Comparison of fuel cell oversizing configurations.

F_D	**1.0**	**1.1**	**1.2**	**1.3**	**1.4**
Variable [Unit]					
OEM [kg]	10,998.7	11,062.4	11,126.2	11,190.4	11,254.7
Payload mass [kg]	3178.7	3115.8	3052.5	2988.6	2924.4
Propulsion system mass [kg]	2922.5	2987.8	3053.1	3118.3	3183.6
LH_2 tank mass [kg]	79.7	78.2	76.8	75.6	74.6
SAF mass [kg]	1436.7	1437.5	1438.3	1439.2	1440.0
Hydrogen mass [kg]	63.5	61.9	60.6	59.5	58.6
Cruise Lift-to-Drag Ratio [-]	13.1060	13.0960	13.0870	13.0760	13.0660
Cruise SAF Flow [kg/s]	0.1170	0.1170	0.1171	0.1172	0.1173
Cruise LH_2 Flow [kg/s]	0.0090	0.0091	0.0089	0.0087	0.0085

Table A2. Comparison of fuel cell cruise oversizing, all configurations have an F_D of 1.4.

Cruise S_P	**0.2**	**0.22**	**0.24**	**0.26**	**0.28**
Variable [Unit]					
OEM [kg]	11,254.7	11,357.2	11,363.0	11,369.7	11,377.1
Payload mass [kg]	2924.4	2925.9	2926.7	2926.7	2927.6
Propulsion system mass [kg]	3183.6	3183.6	3183.6	3183.6	3183.6
LH_2 tank mass [kg]	74.6	81.1	87.9	94.9	101.5
SAF mass [kg]	1440.0	1425.9	1411.9	1398.2	1384.6
Hydrogen mass [kg]	58.6	64.7	71.2	77.9	84.0
Cruise Lift-to-Drag Ratio [-]	13.065	13.089	13.090	13.091	13.093
Cruise SAF Flow [kg/s]	0.117	0.115	0.113	0.110	0.108
Cruise LH_2 Flow [kg/s]	0.009	0.010	0.011	0.012	0.013

References

1. ACARE (Advisory Council for Aviation Research and Innovation in Europe). *Strategic Research & Innovation Agenda: 2017 Update Volume 1*; ACARE: Brussels, Belgium, 2017.
2. Daimler-Benz Aerospace and Airbus GmbH. *CRYOPLANE: Deutsch-Russisches Gemeinschaftsprojekt Flugzeug mit kryogenem Treibstoff*; Daimler-Benz Aerospace and Airbus GmbH: Munich, Germany, 1993.
3. Universal Hydrogen Co. Fueling Carbon-Free Flight. Available online: https://hydrogen.aero/ (accessed on 5 December 2023).
4. ZeroAvia, I. ZeroAvia. Available online: https://zeroavia.com/ (accessed on 5 December 2023).
5. Pornet, C.; Gologan, C.; Vratny, P.C.; Isikveren, A.T.; Hornung, M. Methodology for Sizing and Performance Assessment of Hybrid Energy Aircraft. In Proceedings of the 2013 Aviation Technology, Integration, and Operations Conference, Los Angeles, CA, USA, 12–14 August 2013.
6. Liu, Y. Retrofit and New Design of Regional Aircraft with Hybrid Electric Propulsion. In Proceedings of the AIAA/IEEE Electric Aircraft Technologies Symposium, Denver, CO, USA, 11–13 August 2021.
7. Pontika, E. Integrated mission performance analysis of novel propulsion systems: Analysis of a fuel cell regional aircraft retrofit. In Proceedings of the AIAA SCITECH Forum, National Harbor, MD, USA, 23–27 January 2023. Paper number AIAA 2022-0840.
8. Mandorino, M.; Della Vecchia, P.; Nicolosi, F.; Cerino, G. Regional jet retrofitting through multidisciplinary aircraft design. *IOP Conf. Ser. Mater. Sci. Eng.* **2022**, *1226*, 012047. [CrossRef]
9. Della Vecchia, P.; Mandorino, M.; Cusati, V.; Nicolosi, F. Retrofitting Cost Modeling in Aircraft Design. *Aerospace* **2022**, *9*, 349. [CrossRef]
10. Akshay, J.; Akshay, J.; Sonia, M. Hydrogen Aircraft Market: Global Opportunity Analysis and Industry Forecast, 2030–2040. Available online: https://www.alliedmarketresearch.com/hydrogen-aircraft-market-A08743 (accessed on 5 December 2023).
11. Cambridge University Press & Assessment. Cambridge Dictionary. 2014. Available online: https://dictionary.cambridge.org/de/worterbuch/englisch/retrofit (accessed on 5 December 2023).
12. Lüdemann, M. BLADE: A Modular Environment for Traceable and Automated Aircraft Design. In Proceedings of the 13th EASN International Conference 2023, Salerno, Italy, 5–8 September 2023.
13. Raymer, D. *Aircraft Design: A Conceptual Approach*, 6th ed.; The American Institute of Aeronautics and Astronautics AIAA: Washington, DC, USA, 2018.
14. Torenbeek, E. *Advanced Aircraft Design: Conceptual Design, Analysis, and Optimization of Subsonic Civil Airplanes*; John Wiley & Sons: Chichester, UK, 2013.
15. Airbus Customer Service. *Getting to Grips with Aircraft Performance*; Cedex: Blagnac, France, 2002.
16. DLR (Deutsches Zentrum für Luft- und Raumfahrt). CPACS: A Common Language for Aircraft Design. Available online: https://www.cpacs.de/ (accessed on 30 June 2020).
17. Deutsche Aircraft GmbH: Product D328eco. Available online: https://www.deutscheaircraft.com/products/d328eco (accessed on 5 December 2023).
18. Hein, B. *UMD-Atlas Design Proposal: Heavy Lift Helicopter*; Alfred Gessow Rotorcraft Center: College Park, MD, USA, 2005.
19. Brown, G.V.; Kascak, A.F.; Ebihara, B.; Johnson, D.; Choi, B.; Siebert, M.; Buccieri, C. *NASA Glenn Research Center Program in High Power Density Motors for Aeropropulsion*; NASA (The National Aeronautics and Space Administration): Washington, DC, USA; ARL (United States Army Research Laboratory): Adelphi, MD, USA; 7121 Standard Drive: Hanover, MD, USA, 2005.
20. *Pratt & Whitney Canada PW100 Series Engines: Type-Certificate Data Sheet*; No. IM.E.041; EASA (The European Union Aviaton Safety Agency): Longueuil, QC, Canada, 2023.
21. Wang, L.; Liu, H. Performance studies of PEM fuel cells with interdigitated flow fields. *J. Power Sources* **2004**, *134*, 185–196. [CrossRef]
22. Wang, Y.; Wang, C.Y. Dynamics of polymer electrolyte fuel cells undergoing load changes. *Electrochim. Acta* **2006**, *51*, 3924–3933. [CrossRef]
23. Grujicic, M.; Chittajallu, K.M. Design and optimization of polymer electrolyte membrane (PEM) fuel cells. *Appl. Surf. Sci.* **2004**, *227*, 56–72. [CrossRef]
24. Valle, F. Electrocatalyst Degradation in High Temperature PEM Fuel Cells. Ph.D. Thesis, Università degli studi di Trieste, Trieste, Italy, 2015.
25. Lohse-Busch, H.; Stutenberg, K.; Duoba, M.; Iliev, S. *Technology Assessment of a Fuel Cell Vehicle: 2017 Toyota Mirai*; Energy Systems Division: Argonne, IL, USA, 2018.
26. Teichel, S.H.; Dörbaum, M.; Misir, O.; Merkert, A.; Mertens, A.; Seume, J.R.; Ponick, B. Design considerations for the components of electrically powered active high-lift systems in civil aircraft. *CEAS Aeronaut. J.* **2015**, *6*, 49–67. [CrossRef]
27. Palladino, V.; Jordan, A.; Bartoli, N.; Schmollgruber, P.; Pommier-Budinger, V.; Benard, E. Preliminary studies of a regional aircraft with hydrogen-based hybrid propulsion. In Proceedings of the AIAA Aviation Forum 2021, Virtual, 2–6 August 2021; p. 1587.
28. Gierens, K. Theory of Contrail Formation for Fuel Cells. *Aerospace* **2021**, *8*, 164. [CrossRef]
29. Kellermann, H.; Lüdemann, M.; Pohl, M.; Hornung, M. Design and Optimization of Ram Air–Based Thermal Management Systems for Hybrid-Electric Aircraft. *Aerospace* **2021**, *8*, 3. [CrossRef]
30. Bischoff, T. Development of a Cryogenic Vacuum Insulated Liquid Hydrogen Tank Model. Bachelor's Thesis, Chair of Aircraft Design, TUM (Technische Universität München), Munich, Germany, 2022.
31. Brewer, G.D. *Hydrogen Aircraft Technology*, 1st ed.; CRC Press: Boca Raton, FL, USA, 1991.

32. Flynn, T.M. *Cryogenic Engineering*, 2nd ed.; Revised and Expanded; Marcel Dekker: New York, NY, USA, 2005.
33. Pipes, B. (Ed.) *FLEXWELL CRYO PIPE: Effiziente Lösung für Kryogene Medien*; Adolf-Oesterheld-Straße: Wunstorf, Germany, 2023. Available online: https://www.bruggpipes.com/fileadmin/user_upload/bilder/produkte/05-kryo-anwendungen/BRU_FCP_DatBl_DE_07jul21_FINAL.pdf (accessed on 5 December 2023).
34. Morgan Advanced Materials. *Datenblatt Superwool Blanket*; Thermal Cheramics: Windsor, UK.
35. EASA (The European Union Aviaton Safety Agency). Easy Access Rules for Acceptable Means of Compliance for Airworthiness of Products, Parts and Appliances (AMC-20): SUBPART A—GENERAL. AMC 20-128A Design Considerations for Minimizing Hazards Caused by Uncontained Turbine Engine and Auxiliary Power Unit Rotor Failure. Available online: https://www.easa.europa.eu/en/document-library/easy-access-rules/online-publications/easy-access-rules-acceptable-means?page=23 (accessed on 5 December 2023).
36. Viguier, C. *IMOTHEP Internal Report RA5.2: Report on Static Optimized EPU Subsystem and Components along Requirements of Vehicle Designs L1*; Safran Group: Paris, France, 2022.
37. Habermann, A.L.; Kolb, M.G.; Maas, P.; Kellermann, H.; Rischmüller, C.; Peter, F.; Seitz, A. Study of a Regional Turboprop Aircraft with Electrically Assisted Turboshaft. *Aerospace* **2023**, *10*, 529. [CrossRef]
38. Zschocke, A.; Scheuermann, S.; Ortner, J. *High Biofuel Blends in Aviation (HBBA): Final Report*; ENER/C2/2012/420-1; Lufthansa: Cologne, Germany, 2017.
39. Hypoint. Technical White Paper. 2021. Available online: https://docsend.com/view/t9aw2mk (accessed on 15 December 2021).